Am J Transl Res 2022;14(2):1361-1375
www.ajtr.org /ISSN:1943-8141/AJTR0135433

Original Article

Over-expression of miR-193a-3p regulates the apoptosis of colorectal cancer cells by targeting PAK3

Tao Ma[1], Hai Li[2], Wenjing Yang[1], Quanxia Liu[1], Hui Yan[1]

[1]*The Second Department of Oncology, Tumor Hospital, General Hospital of Ningxia Medical University, Yinchuan 750004, Ningxia, People's Republic of China;* [2]*The Colorectal Surgery, General Hospital of Ningxia Medical University, Yinchuan 750004, Ningxia, People's Republic of China*

Received May 19, 2021; Accepted November 4, 2021; Epub February 15, 2022; Published February 28, 2022

Abstract: Although dysregulated expression of microRNAs (miRNA) has been investigated in colorectal cancer (CRC), MiR-193a-3p, as a tumor inhibitor, is less studied. To investigate the function and mechanism of miR-193a-3p in CRC, the potential function of miR-193a-3p in regulating PAK3 in CRC with a series of experimental assays including western blotting, qRT-PCR, bioinformatics analysis, a luciferase reporter assay, flow cytometry, Transwell assay, CCK8 assay and immunofluorescence were performed in this study. The results showed that miR-193a-3p was down-regulated in CRC tissues and cell lines, which was also correlated with tumor progression. PAK3 was predicted as a target gene of miR-193a-3p in CRC cells by TargetScan database, which was confirmed by luciferase assays. Moreover, overexpression of miR-193a-3p suppressed the viability, cell cycle progression, migration, and invasion, and induced apoptosis of CRC cells *in vitro* by regulating the PAK3 signaling pathway. Therefore, miR-193a-3p may serve as a tumor suppressor and potential target for CRC treatment.

Keywords: miR-193a-3p, colorectal cancer, PAK3, regulate, apoptosis

Introduction

Colorectal cancer (CRC) is the second dominant cause of cancer-associated death globally [1, 2]. Tremendous achievements have been reported in multiple CRC therapeutic strategies recently, including surgical removal, chemo- and immuno-therapy [3, 4]. Despite the improvement in past years, CRC is yet incurable, mainly due to its invasion and metastasis after treatment [5, 6]. Searching for efficient targets is still the main goal in the research field due to the considerable potential of targeted treatment. The occurrence and progression of CRC involve the stimulation of proto-oncogenes and the deactivation of tumor inhibition genes, as well as variations of microRNAs (miRNAs) in the tumor microenvironment [7, 8]. MiRNAs is a group of non-coding RNAs, which consist of 22 nucleotides and modulate the gene expression by binding to the 3'-untranslated region (UTR) of their target mRNAs [9, 10]. MiRNAs have significant functions in many cell biology processes such as proliferation, migration, apoptosis, spread and division [11, 12]. Many miRNAs may play oncogenic or suppressive role by modulating their downstream targets in the CRC development [13-15]. For instance, miR-107 inhibits the division, movement, and invasion of SW620 cells by negatively mediating transferrin receptor-1 [16]. MiR-6716-5p crucially regulates NAT10 to facilitate cell motion and metastasis in CRC [17]. MiR-21, -143, -370 and -193a-3p also contribute to CRC procession, but the mechanisms are still not clear [18-20].

MiR-193a-3p could target CCND1 to inhibit the development of pancreatic ductal adenocarcinoma (PDAC) cells, thus providing a potential treatment and prognostic target for PDAC [21]. Overexpression of miR-193a/b-3p relieves hepatic fibrosis by restricting the division and migration of hepatic stellate cells, which suggests that miR-193a-3p and -193b-3p could be new treatment targets for hepatic fibrosis [22]. P21-activated kinase 3 (PAK3) is a member of Rac/Cdc42-related serine/threonine

Table 1. Associations between miR193a-3p and PAK3 expression levels and clinicopathological characteristics of patients with CRC

Features	cases n=40	miR-193a-3p		*P* value	PAK3 mRNA		*P* value
		High, n=16	Low, n=24		High, n=19	Low, n=21	
Gender				0.517			0.062
Female	15	5	10		10	5	
Male	25	11	14		9	16	
Age, years				0.531			0.119
≤60	20	7	13		12	8	
>60	20	9	11		7	13	
Differentiation				0.531			0.355
Well	20	7	13		11	9	
Moderate, poor	20	9	11		8	12	
Tumor size, cm				0.446			0.504
≤4	17	8	9		7	10	
>4	23	8	15		12	11	
TNM stages				<0.001			0.050
I, II	17	12	5		5	12	
III	23	4	19		14	9	
Lymph node metastasis				<0.001			0.209
No	19	13	6		7	12	
Yes	21	3	18		12	9	

P<0.05 indicates statistically significant difference; High, high expression; Low, low expression.

protein kinases, which is pivotal in many cellular processes such as cell migration, proliferation, apoptosis, cytoskeletal rearrangement, and vessel formation [23]. In addition, many studies have stated that the abnormal expression of miR-193a-3p and PAK3 plays a role in the metastasis of multiple cancers such as breast cancer, gastric cancer and so on [24-26]. However, the relationship between CRC and PAK3 has not been investigated. Actually, the prediction using TargetScan has revealed that the 3'-UTR of PAK3 mRNA contains the potential binding sites to miR-193a-3p. The primary study here implied the modulating role of miR-193a-3p in the PAK3 expression. Therefore, it's hypothesized that the over-expression of miR-193a-3p could regulate the apoptosis of colorectal cancer cells by targeting PAK3.

Materials and methods

Clinical samples

A total of forty CRC tissues and matched surrounding tissues were obtained from patients who received colon resection from May 2015 to Feb 2017 at Tumor Hospital, General Hospital of Ningxia Medical University in China. All tissues were from patients participated in a randomized controlled trial. Inclusion criteria: (1) CRC patients were diagnosed by at least two experienced pathologists; (2) patients had complete clinical information and follow-up data. Exclusion criteria: (1) patients had other malignant tumor history or treatment history; (2) patients underwent chemo- or radio-therapy before surgery. Approval was given by the ethics committee of our hospital, and written informed consent was provided by all participants. The clinicopathological features of patients are summarized in **Table 1**.

Cell culture

CRC cell lines SW480, SW620, HCT116, DLD1, and Caco2 and the normal cell line CCD-18Co were bought from the Cell Resource Center of the Academy of Sciences (Beijing, China). All cells were grown in DMEM supplemented with 10% FBS (Gibco; Thermo Fisher Scientific, USA), 100 mg/ml streptomycin and 100 U/ml penicillin at 37°C and in 5% CO_2.

Immunohistochemical (IHC) analysis

In brief, the tested tissues fixed with formalin and embedded with paraffin were cut into 4 μm-thick sections. The sections were treated

with xylene and a gradient of ethanol, cultured with 3% H_2O_2 for 30 min, and blocked with 3% bovine serum albumin for 1 h. Then incubation was conducted first with an anti-PAK3 antibody (cat. no. 21401-1-AP, 1:200) overnight at 4°C, and then with biotin-conjugated affinipure goat anti-rabbit IgG (H+L) (SA00004-2, 1:6000) (both proteintech, Proteintech Group, USA). Immunostaining was tested with a Nikon Eclipse TI-SR light microscope (Nikon Corporation; 200×). Semi-quantitative immunoreactivity score (IRS) was calculated separately by two diagnosticians by multiplying the quantity and intensity scores. Typically, 0-25%, 26-50%, 51-75%, and 76-100% immunoreactive cells were assigned with a quantity score of 1 to 4 respectively. Moreover, negative, weak, moderate, and strong immunostaining corresponded to the intensity score of 0 to 3 respectively. Finally, within a range from 0 to 12, IRS of 0, 1-4, 5-8 and 9-12 were classified as -, +, ++ and +++ respectively. Moreover, - and + were regarded as low-expression, and ++ and +++ as high-expression.

In situ hybridization (ISH)

ISH was used to detect miR-193a-3p in tissues using digoxigenin-labeled sense and antisense miR-193a-3p probes (Sangon, China). The slides were de-paraffined and rehydrated before incubation with Proteinase K at 37°C for 40 min, and then washed three times with PBS for 15 min. After incubation with 5× SSC solution at room temperature for 15 min, miR-193a-3p probes were added for hybridization at 50°C for 1 h. Next, the slides were washed with graded-diluted SSC solutions at 50°C for 30 min, followed by incubation with an antibody against digoxigenin (1:1000, Roche, Mannheim, Germany) at 4°C overnight. Finally, slides were counterstained with nuclear fast red for 1 min and then mounted using an aqueous solution.

Cell transfection

SW620 and DLD1 cells pre-seeded in 6 well plates were first transfected with miR-193a-3p mimics or inhibitors (100 nM) and PAK3 small interfering (si)RNA (50 nM) (GenePharma Company, http://www.genepharma.com/about.php), and then transfected with pcPAK3 or pcDNA (negative control) using Lipofectamine 3000 reagent (Invitrogen; Thermo Fisher Scientific, Inc.), according to the manufacturer's instructions. Cells were cultured at 37°C for 24 h following the last transfection before downstream tests. The sequences of siRNAs, mimics and inhibitors are listed in Table S1.

RT-qPCR

Total RNA was isolated from tissues and CRC cell lines with TRIzol agents (Invitrogen; Carlsbad, CA, USA) as per the manufacturer's instruction, and was reverse-transcribed into cDNA with BeyoRT™ II M-MLV agents (cat. no. D7160L, Beyotime). QPCR was carried out on a 7500 Applied Biosystems PCR system (Thermo Fisher Scientific) with a BeyoFast™ SYBR Green qPCR mix kit (cat. no. D726, Beyotime). The forward and reverse primers are listed in Table S2. U6 was used as the internal control. The cycling program was: 95°C, 10 min; 36 cycles of 95°C, 20 sec and 60°C, 1 min. Relative expression was calculated using $2^{-\Delta\Delta Ct}$ method [27]. All tests were repeated three times.

Luciferase assays

TargetScan 7.2 (www.targetscan.org) and miRDB (www.mirdb.org) were used to predict potential target genes of miR-193a-3p. The PCR-amplified products of the 3'-UTRs of PAK3 (transcript variant 25) were gel-purified, digested and placed into a pGL3-basic vector (Promega, Madison, WI, USA). The primer sequences are listed in Table S3. Site-directed mutations were generated by PCR with suitable primers containing desired mutations. The site-directed mutations were completed by commercial service and primer information was not given (Sangon Biotech, Shanghai). All constructs were verified by sequencing.

As for the luciferase assays, SW620 and DLD1 cells were temporally transfected with 0.1 μg of reporter plasmid and 0.65 pmol miRNA mimics or inhibitors in 96-well plates. After 48 h, assays were carried out on a dual-luciferase reporter assay system (Promega, Madison, WI, USA). The luciferase activity was standardized with *Renilla* luciferase as a control. All assays were conducted in triplicate.

Cell viability assay

After transfection, the viability of CRC cells was detected by a cell counting kit-8 (cat. no.

C0037, Beyotime) as per the protocol. In brief, 2×10^3 cells/well were seeded into 96-well plates for 12, 24, 48 or 72 h, and each well contained 100 μl of DMEM (Gibco; Thermo Fisher) with 10% FBS and 100 U/ml penicillin. Afterwards, the CCK-8 assay reagent (10 μl) was added to each well mixed with the medium without serum (90 μl). After 2 h, the absorbance at 450 nm was detected by a microplate reader.

Migration and invasion assays

The migration and invasion of CRC cells were tested via Transwell assays. The filters (Corning Incorporation, NY, USA) were cleaned in serum-free DMEM and put into 12-well plates. The transfected CRC cells (3×10^4 cells) planted in 200 μl of a serum-free medium were grown in the top chamber with or without 2 mg/ml matrigel-coated films with 8-μm pores (BD Biosciences, Franklin Lakes, NJ, USA), while the lower chamber was added with 700 μl of the base medium with 10% FBS. After 24 h, the cells were methanol-fixed, and the upper-chamber cells were swabbed. The lower-chamber cells were dyed with a 0.1% crystal violet solution (cat. no. C0121, Beyotime) and photographed in 5 random zones under an inverted microscope (Nikon Corporation, Otsu, Japan). The mean cell count in the 5 zones was adopted for quantitative tests. Each assay was repeated three times.

Cell cycle analysis

CRC cells were transfected with miR-193a-3p mimics or inhibitors, harvested, cleaned, and resuspended into PBS following treatment with 0.25% trypsin for 2 min at 37°C and fixation in 70% ethanol at -20°C overnight. Next, the cells were cleaned with PBS twice and cultured in a buffer containing propidium iodide (PI) (cat. no. C1052, Beyotime) at room temperature for 15 min. Finally, the cells were analyzed using BD FACSCalibur with a four-color fluorescence detection system and Modfit LT 4.1 (Verity Software House, Inc., Topsham, ME, USA).

Apoptosis assay

CRC cells were transfected with miR-193a-3p mimics or inhibitors for 48 h, and then collected and washed with PBS twice at 37°C. The apoptosis of transfected cells was determined by an apoptosis detection kit (cat. no. C1062M, Beyotime) following the manufacturer's protocol. Briefly, the cells were re-suspended in an Annexin V-FITC and PI solution (cat. no. C1062M, Beyotime) for 30 min in the dark at 37°C. Then, after the addition of an Annexin V binding solution, the cells were detected with BD FACSCalibur with the four-color fluorescence system (BD Biosciences). Quantification with flow cytometry uncovered the cell fractions in the early and late stages of apoptosis. All tests were carried out in triplicate.

Flow cytometry of CD73 and CD133

CRC cells transfected with miR-193a-3p mimics or inhibitors for 24 h were collected and washed twice with PBS containing 0.2% BSA. Then the cells were stained at 37°C for 30 min with phycoerythrin-marked monoclonal CD73 (cat. no. FAB5795P, 1:100, R&D Systems, Inc. USA) or allophycocyanin-marked CD133 (cat. no. MAB11331-SP, 1:200, R&D Systems, Inc. USA) antibodies or the isotype controls (dilution, 1:200; cat. no. 560787; BD Biosciences) at 37°C for 30 min. After cleaning twice with PBS and fixing in 10% (v/v) formaldehyde-PBS at 37°C, the cells were arranged and observed using a BD FACSC alibur with the four-color fluorescence system (BD Biosciences). Statistical analyses were carried out on FlowJo 7.6. Average fluorescence intensity and positive cell percent were computed by subtracting the data of the controls.

Apoptosis analysis by immunofluorescence

Cells transfected with the mimics or inhibitors for 24 h were cleaned with PBS twice, dyed with Hoechst 33258 (100 μl) (cat. no. C1011, Beyotime) and cultured in dark at 37°C for 30 min. Afterwards, the cells were cleaned, resuspended with PBS, watched with a fluorescence microscope (×200; Nikon, Tokyo, Japan) and detected on a DP2-BSW system. The chromatin of dead cells was concentrated.

Western blot

The transfected cells were lysed for protein quantification via a BCA method. The proteins (20 μg) were isolated by 10% SDS-PAGE and removed onto PVDF films (Bio-Rad, Hercules, USA). The films were cultured first with primary antibodies against PAK3 (cat. no. 14092-1-AP, 1:2000, Proteintech, USA), caspase-9 (cat. no. 10380-1-AP, dilution 1:800), Apaf-1 (cat. no. 21710-1-AP, 1:5000), caspase-3 (cat. no. 19677-1-AP, 1:1000) and GAPDH (cat. no.

10494-1-AP, 1:2000) at 37°C for 60 min, and then with HRP-conjugated affinipure goat anti-rabbit IgG (H+L) (cat. no. SA00001-2, 1:6000). GAPDH served as a control. Grey value of protein band was determined with ImageJ software.

Statistical analysis

All data and results were analyzed using SPSS 16.0 (SPSS, Chicago, USA) and GraphPad 5.0 (GraphPad, La Jolla, USA). Categorical data were compared via either Chi-square test or Fisher's exact test, while continuous data were examined via Student's t-test, Mann-Whitney U test, or one-way analysis of variance with Tukey's post hoc test. All tests were done in triplicate. CRC patients were separated into high and low expression of miR-193a-3p groups in line with the mean value of miR-193a-3p expression and survival analysis between groups was performed by Kaplan-Meier curves and compared with log-rank test. The significant level was set at $P<0.05$.

Results

The accumulation of MiR-193a-3p and PAK3 in CRC tissues and cells

To understand the functions of miR-193a-3p and PAK3 in CRC cells, we first detected the accumulation of miR-193a-3p and PAK3 in CRC cells and tissues. We found that the level of miR-193a-3p expression was lower in primary CRC tissues compared to that in adjacent noncancerous tissues ($P<0.001$; **Figure 1A**). However, the mRNA levels of PAK3 were upregulated in cancer tissues when compare with those in normal tissues ($P=0.008$; **Figure 1B**). The mRNA levels of PAK3 were inversely associated with miR-193a-3p expression in tumor tissues (Pearson r=-0.488, $P=0.006$; **Figure 1C**). The mean level of miR-193a-3p expression in tumors was used to divide cases into two groups (high and low groups). The low expression of miR-193a-3p indicated the poor clinical outcome of patients (log rank test, $P=0.047$; **Figure 1D**). Furthermore, the protein levels of PAK3 in CRC tissues were evaluated and the results showed that PAK3 proteins were increased in CRC samples (**Figures 1E** and S1). The results of ISH analysis demonstrated that miR-193a-3p was significantly lower in tumor tissues than that in normal control tissues (**Figure 1F**). Besides, we found that the expression level of miR-193a-3p was downregulated in SW480, SW640, HCT116, DLD1, and Caco2 cells (**Figure 1G**). Conversely, both the mRNA and protein of PAK3 were overexpressed in CRC cell lines (**Figure 1H-J**). The dysregulated miR-193a-3p and PAK3 may have roles in the development of CRC.

Abnormalities of MiR-193a-3p and PAK3 were associated with clinicopathological features of patients

To reveal the clinical relevance of miR-193a-3p and PAK3 in CRC, the mean levels of miR-193a-3p and PAK3 mRNA in CRC tissues were used as cut-off value to divide cases into high- and low-expression groups. We found that the reduced miR-193a-3p expression was significantly correlated with advanced TNM stage and lymph node metastasis ($P=0.006$ and 0.001, respectively), but not with gender, age or tumor size (all $P>0.05$, **Table 1**). The mRNA expression of PAK3 was not correlated with clinicopathological features of patients, which could be due to the limited patient samples.

PAK3 was a target of MiR-193a-3p in CRC cells

Bioinformatics analysis showed that miR-193a-3p has potential binding sites in the 3'-UTR of PAK3 mRNA (**Figure 2A**). A total of four binding sites (two highly conserved and two poorly conserved) were predicted. We selected the position 255-261 of PAK3 3'UTR (the conserved and the first proximal binding site) for further bioinformatics analysis. The wild-type or mutant 3'-UTR sequences of PAK3 containing the binding sites of miR-193a-3p were cloned into pGL3 plasmids. The luciferase reporter assay displayed that the induced expression of miR-193a-3p inactivated the luciferase of PAK3-WT, but not PAK3-MUT, in SW620 cells (**Figure 2B**), which implied the reliable connection between PAK3 and miR-193a-3p. The mRNA and protein levels of PAK3 were inhibited by miR-193a-3p mimics, while increased by miR-193a-3p inhibitors (**Figure 2C** and **2D**). Similarly, the luciferase activity of PAK3 3'-UTR was suppressed by miR-193a-3p in DLD1 cells (**Figure 2E**). The mRNA and protein expression of PAK3 was negatively regulated by miR-193a-3p (**Figure 2F** and **2G**). The expression of PAK3 protein decreased significantly in si-PAK3 + miR-193a-3p inhibitors transfected cells and increased in miR-193a-3p mimics + pc-PAK3 transfected cells (**Figure 2H**). These results indicate that

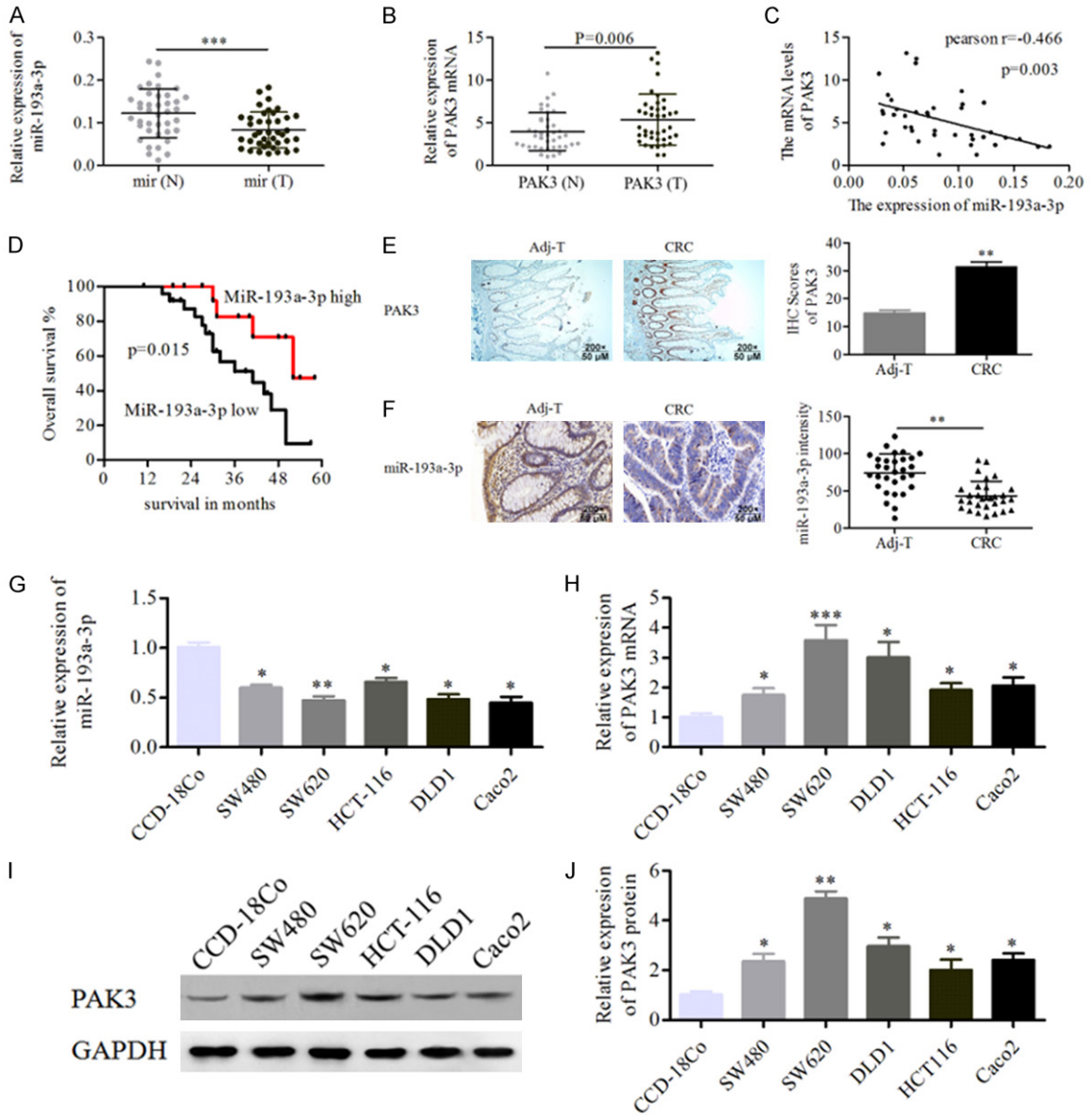

Figure 1. Expression of miR-193a-3p and PAK3 in CRC tissues and cell lines. A. MiR-193a-3p was downregulated in CRC tissues (adjacent normal tissues *vs.* CRC tissues). B. The mRNA expression of PAK3 in CRC tissues was measured by qRT-PCR assay (adjacent normal tissues *vs.* CRC tissues). C. The mRNA expression of PAK3 was negatively correlated with miR-193a-3p in tumors. D. Low expression of miR-193a-3p was associated with the poor prognosis. E. Representative IHC staining of PAK3 in CRC tissues. F. ISH assay for the expression of miR-193a-3p in CRC tissues. G and H. The expression of miR-193a-3p and PAK3 mRNA in CRC cell lines (normal control cells *vs.* CRC cells). I and J. The protein expression of PAK3 in CRC cells (normal control cells *vs.* CRC cells). CRC cell lines: SW480, SW620, HCT116, DLD1, Caco2. Normal cell line: CCD-18Co. Statistical significance: $^{*}P<0.05$, $^{**}P<0.01$, $^{***}P<0.005$.

PAK3 is a novel target of miR-193a-3p in CRC cells.

MiR-193a-3p inhibited cell proliferation and induced cell cycle arrest and apoptosis

The miR-193a-3p in CRC cells was overexpressed and knocked down by the transfection with miR-193a-3p mimics and inhibitors, respectively. The results of CKK-8 assay showed that miR-193a-3p overexpression inhibited the proliferation of SW620, DLD1 and HCT-116 cells (**Figure 3A**). The effects of miR-193a-3p on cell cycle and apoptosis were assessed through Flow cytometry, which displayed that up-regulation of miR-193a-3p sig-

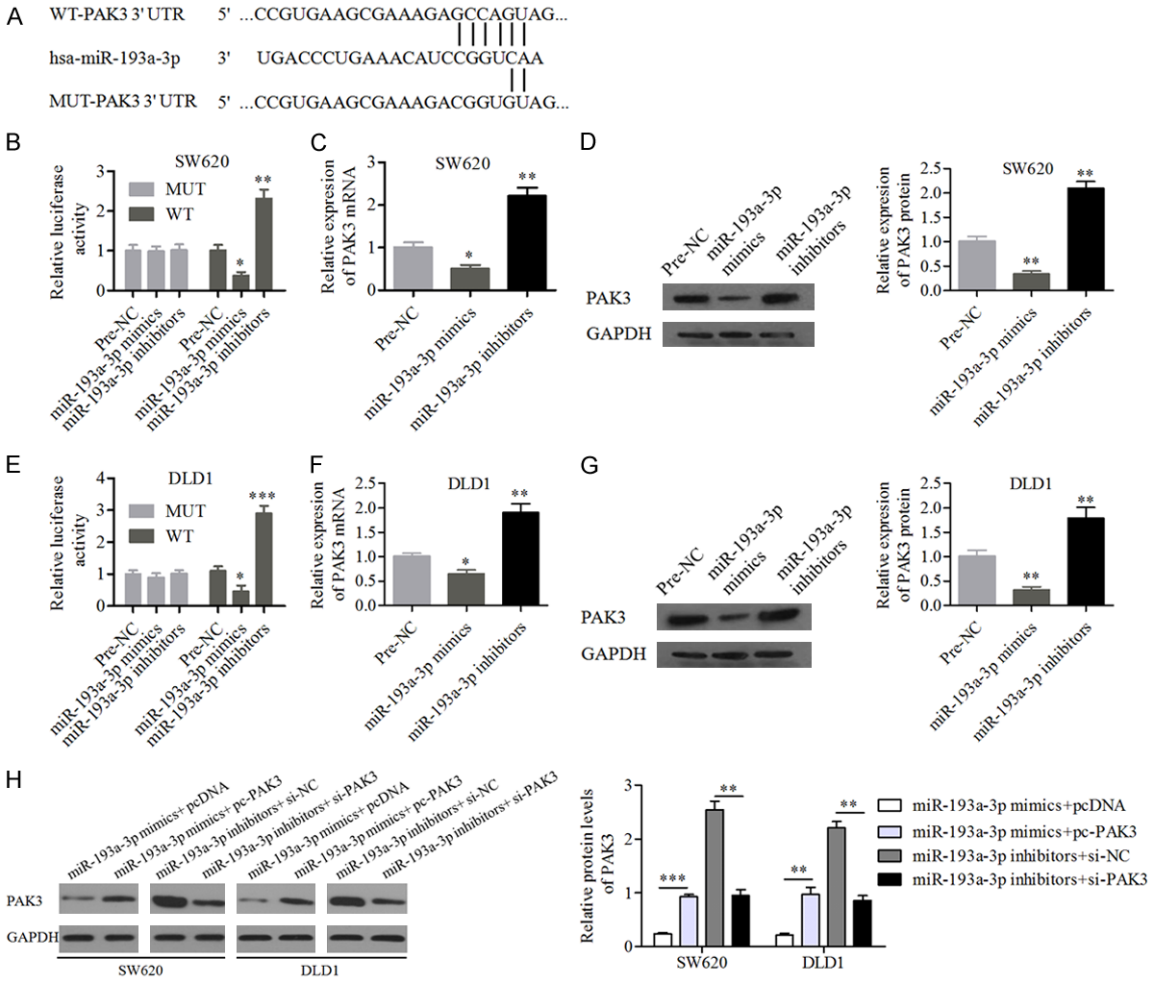

Figure 2. PAK3 was proved to be a direct target of miR-193a-3p. A. The first proximal and conserved binding sites of miR-193a-3p on PAK3 mRNA 3'-UTR. B and E. The luciferase activity of the wild type target sequences (WT), but not the mutant type (MUT), was suppressed by miR-193a-3p mimics. C, D, F and G. The mRNA and protein levels of PAK3 were negatively regulated by miR-193a-3p in SW620 and DLD1 cells. H. PAK3 was validated as a direct target of miR-193a-3p in DLD1 cells. CRC cell lines: SW620, DLD1. Statistical significance: $^{*}P<0.05$, $^{**}P<0.01$, $^{***}P<0.005$.

nificantly increased the apoptosis of SW620, DLD1 and HCT-116 cells (**Figure 3B**). In addition, knockdown of miR-193a-3p reversed the apoptosis of CRC cells (**Figure 3B**). The results of cell cycle analysis revealed that miR-193a-3p overexpression significantly increased the cells in G0/G1 phase (**Figure 3C**), whereas knockdown of miR-193a-3p induced the cell gathering at stages S and G2 in CRC cells (**Figure 3C**).

MiR-193a-3p regulated the expression of apoptosis-related proteins

In order to further validate the influence of miR-193a-3p on apoptosis, we stained the transfected CRC cells with Hoechst 33258. We found that overexpression of miR-193a-3p increased cell apoptosis but silencing of miR-193a-3p restrained the apoptosis of CRC cells (**Figure 4A** and **4B**). Since there was a regulatory role of miR-193a-3p in apoptosis, we analyzed the apoptosis-related proteins caspase-3/9 and Apaf-1 in CRC cells. The results of Western blot revealed that the protein expression of caspase-3/9 and Apaf-1 was upregulated by miR-193a-3p mimics and downregulated by miR-193a-3p inhibitors (**Figure 4C**). These data indicate that miR-193a-3p affects cell apoptosis through regulating the expression of apoptosis-related proteins.

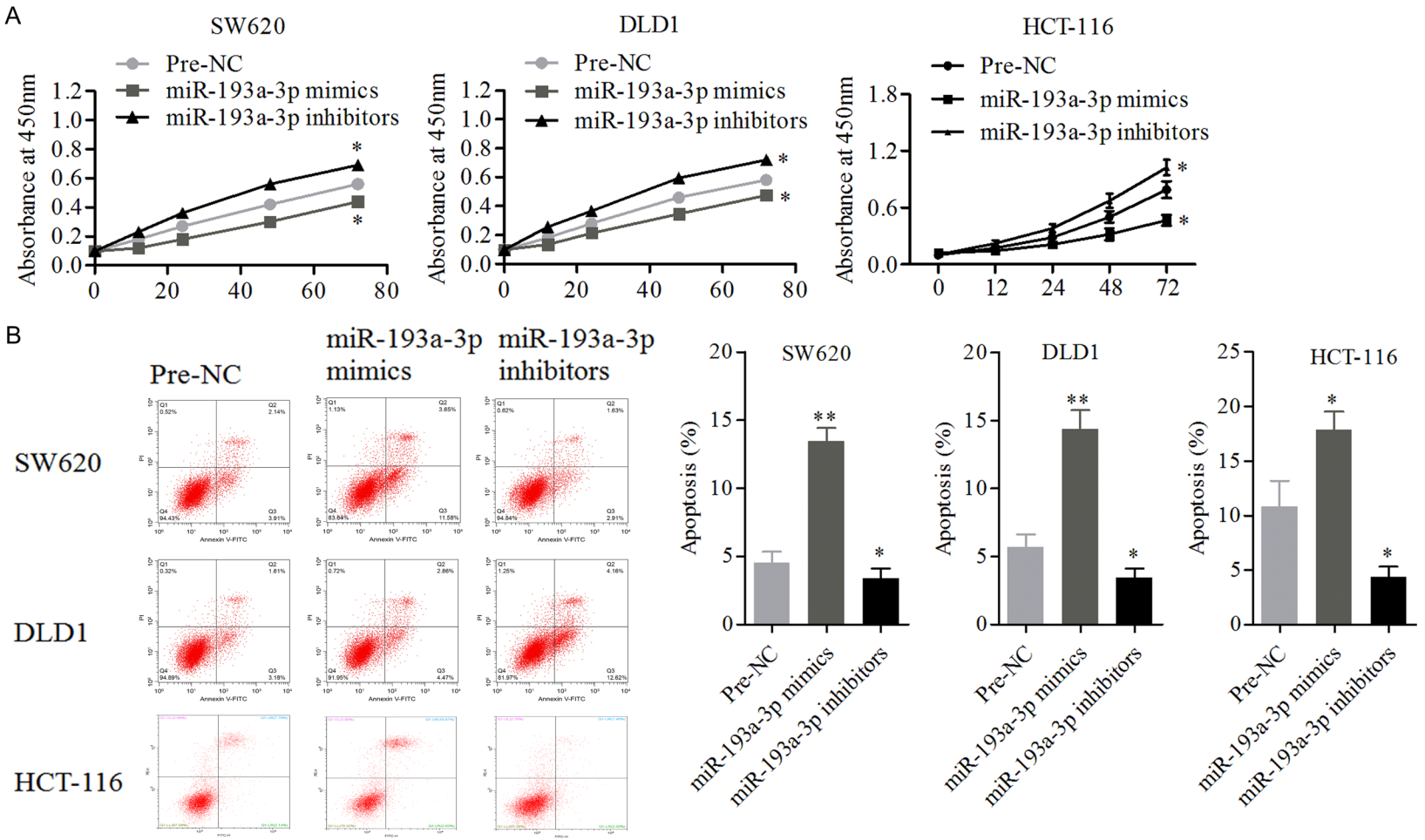
A
SW620
DLD1
HCT-116
Pre-NC
miR-193a-3p mimics
miR-193a-3p inhibitors
Absorbance at 450nm
B
Pre-NC
miR-193a-3p mimics
miR-193a-3p inhibitors
SW620
DLD1
HCT-116
Annexin V-FITC
PI
Apoptosis (%)

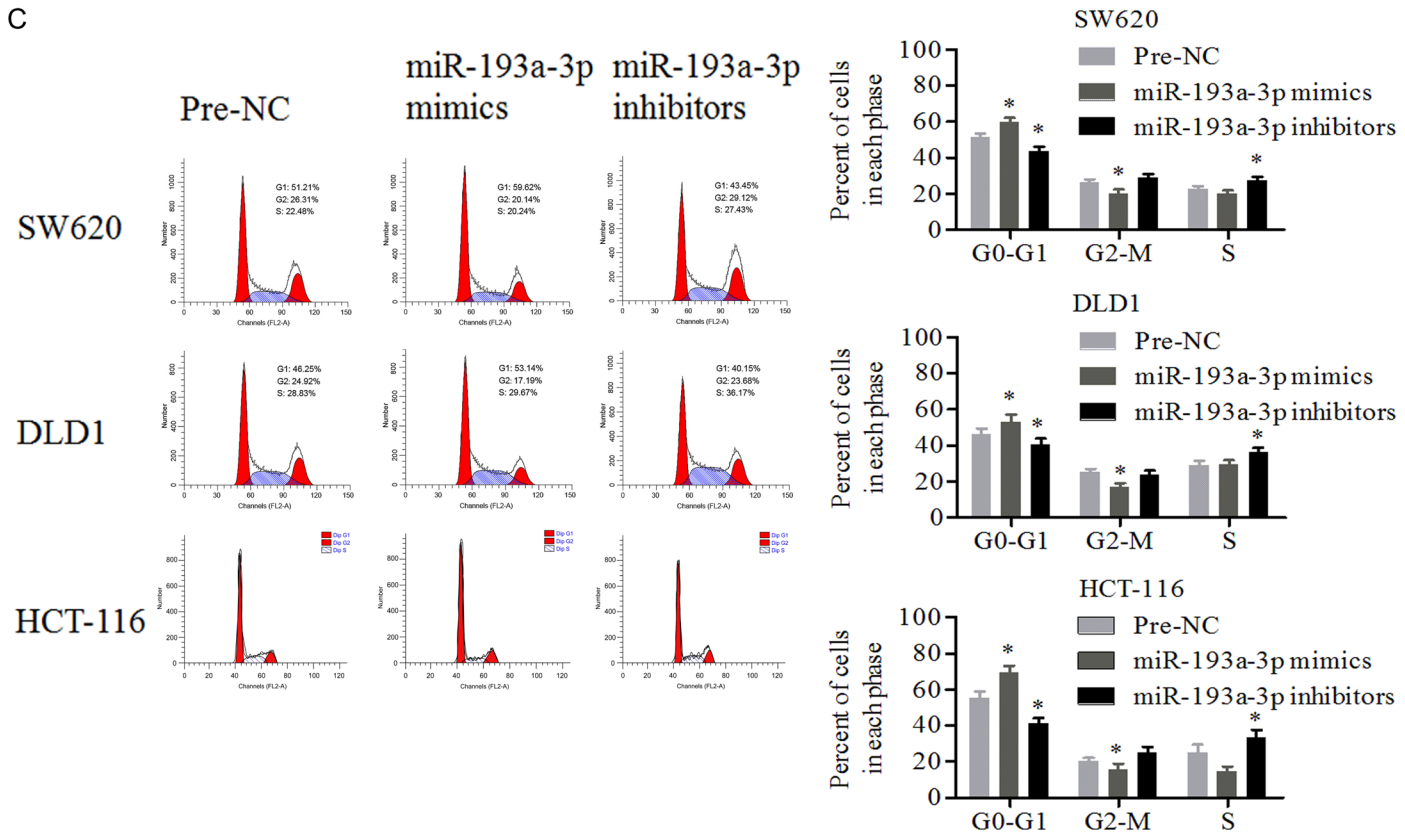

Figure 3. MiR-193a-3p inhibited cell proliferation, cell cycle and enhanced cell apoptosis. A. MiR-193a-3p inhibited the proliferation of CRC cells *in vitro* as analyzed using CCK-8 assay. B. Overexpression of miR-193a-3p increased the number of apoptotic cells, while knockdown of miR-193a-3p decreased the apoptotic cells. C. Cell cycle distribution of CRC cells was analyzed by Flow cytometer. CRC cell lines: SW620, HCT116, DLD1. Statistical significance: $^{*}P<0.05$, $^{**}P<0.01$, $^{***}P<0.005$.

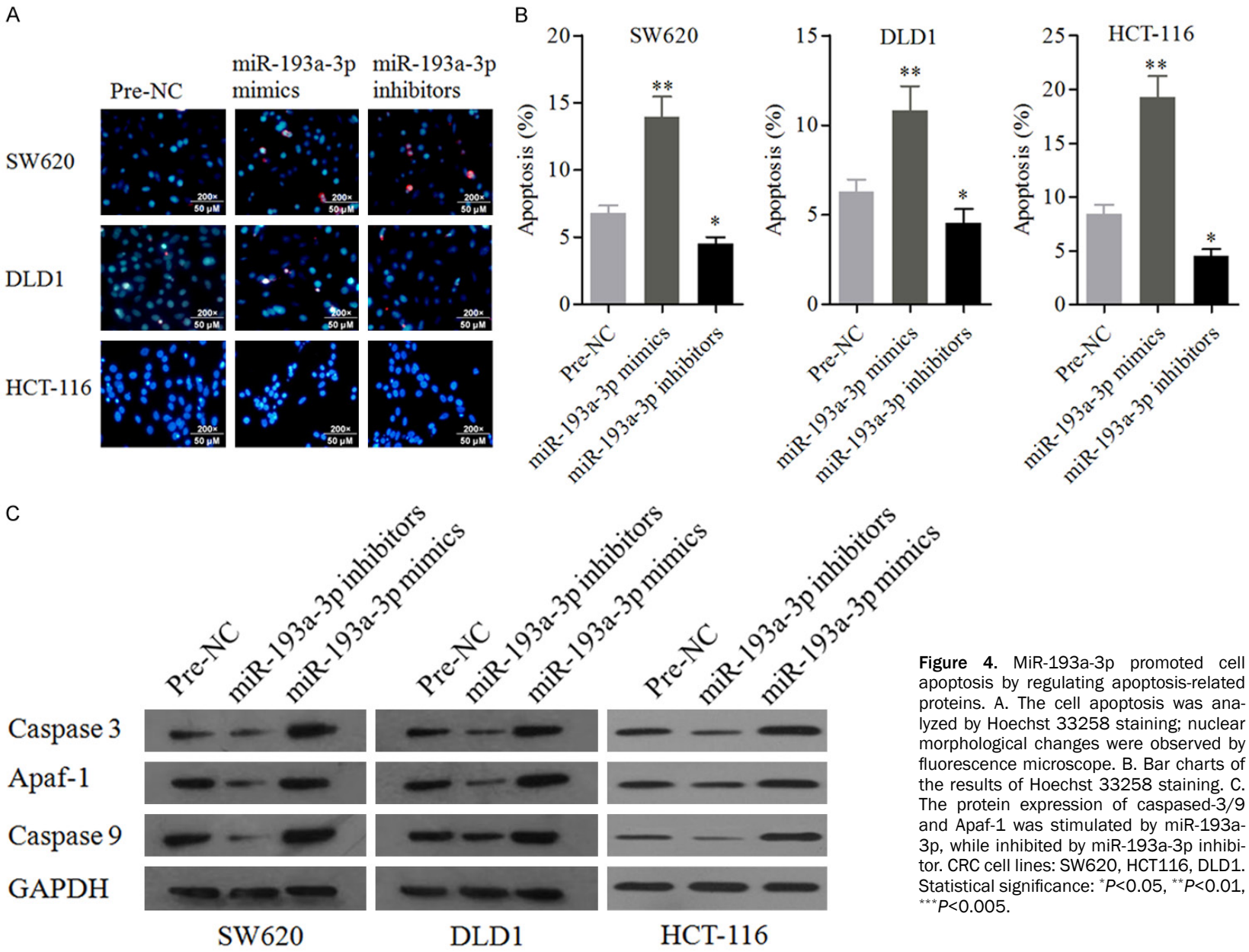

Figure 4. MiR-193a-3p promoted cell apoptosis by regulating apoptosis-related proteins. A. The cell apoptosis was analyzed by Hoechst 33258 staining; nuclear morphological changes were observed by fluorescence microscope. B. Bar charts of the results of Hoechst 33258 staining. C. The protein expression of caspased-3/9 and Apaf-1 was stimulated by miR-193a-3p, while inhibited by miR-193a-3p inhibitor. CRC cell lines: SW620, HCT116, DLD1. Statistical significance: $^{*}P<0.05$, $^{**}P<0.01$, $^{***}P<0.005$.

MiR-193a-3p suppressed cell migration and invasion in vitro

The effect of miR-193a-3p on cell migratory and invasive ability was measured using Transwell assay. The migratory ability of CRC cells was suppressed by miR-193a-3p mimics and elevated by miR-193a-3p inhibitors (**Figure 5A**). Likewise, ectopic expression of miR-193a-3p repressed cell invasiveness, while knockdown of miR-193a-3p exerted the opposite effect on cell invasion (**Figure 5B**). These results suggest that miR-193a-3p can suppress the motility of CRC cells.

Analysis of CD73 and CD133 on cell surface

The protein expression of CD73/133, which is related to the invasion and metastasis of cancer cells, was detected in SW620, DLD1 and HCT-116 cells transfected with miR-193a-3p mimics or inhibitors. We found that CD73/133 were up-regulated in the miR-193a-3p mimics transfected cells and reduced in inhibitors-transfected cells (**Figure 5C** and **5D**), indicating that the expression of miR-193a-3p influenced the expression of CD73 and CD133 to regulate the invasion and the metastasis of CRC cells.

Discussion

Recently, tremendous investigations have implied important roles of miRNAs in pathological processes of many cancers, such as proliferation, migration, invasion, angiogenesis, and apoptosis [28, 29]. MiRNAs have been suggested not only as the prognostic factors and biomarkers for various cancers, but also as potential therapeutic targets for cancers. MiR-193a-3p was first investigated in parietal cells in 2003 as a tumor inhibitor and transforming factor [30]. MiR-193a-3p located at 16p13 is involved in pathological processes of cancers by acting as a key oncogene and regulator. However, many studies also state the tumor suppressing role of miR-193b in distinct cancers. For instance, miR-193b suppressed tumor growth through different tumorigenic routes and was significantly down-regulated in hepatocellular carcinoma tissues [31]. MiR-193a-3p was also discovered as a new tumor inhibitor in T-cell acute lymphoblastic leukemia by targeting MYB [32]. Moreover, miR-193b was significantly down-regulated and played anti-tumorigenic roles in gastric cancer cells by targeting cyclin D1 [33]. Nevertheless, the molecular mechanisms and functions of miR-193a-3p in CRC progression are still unclear. The result in this study displayed that miR-193a-3p was aberrantly down-regulated in CRC tissues and cell lines.

It is well known that the over-expression of PAK3 in thymic carcinoids facilitated cell invasion and movement, which indicates that there is a possible relationship between tumor formation and PAK3 [34]. However, there are few researches that studied the expression of PAK3 in CRC. In this study, the PAK3 was found with excessive expression in CRC tissues and cell lines. Bioinformatics analysis showed that PAK3 was the target gene of miR-193a-3p, as verified by luciferase assays after the transfection with miR-193a-3p inhibitors and mimics. The results indicated that over-expression of miR-193a-3p restricted the expression of PAK3, and down-expression of miR-193a-3p increased PAK3 expression. Although group I PAKs, including PAK1/2/3, share 80-90% sequence identity within the catalytic zones [35], the abnormal expression of miR-193a-3p cannot affect the expression of PAK1 and PKA2, which is consistent with the bioinformatics prediction. In addition, the PAK3 knockdown mediated by the miR-193a-3p overexpression impeded the growth, migration and invasion of CRC cells. Meanwhile, miR-193a-3p overexpression led to cell cycle arrest at G1 phase to suppress cell proliferation.

CD73 and CD133 play functional roles in solid tumors through various mechanisms such as tumor milieu immune inhibition, transfer, anti-chemotherapy, and vasculogenesis. CD73 is expressed in multiple cancers, and its high expression in tumor tissues is related to low overall and recurrence-free survival rates in patients with breast or ovarian cancer [36]. As a biomarker for division and characterization of stem cells, CD133 could be pivotal in cell progression, growth, and pathophysiology of growing tumors [37]. We found that over-expression of miR-193a-3p restricted the expression of CD73 and CD133 in CRC cells by targeting PAK3 and inhibited the metastasis of CRC *in vitro*.

Caspase-9 and caspase-3 both belong to the caspase family, which are involved in the apoptosis process. Caspase-9 is involved in and stimulated cells into apoptotic parts at a multi-protein level [38]. Caspase-3 is a critical

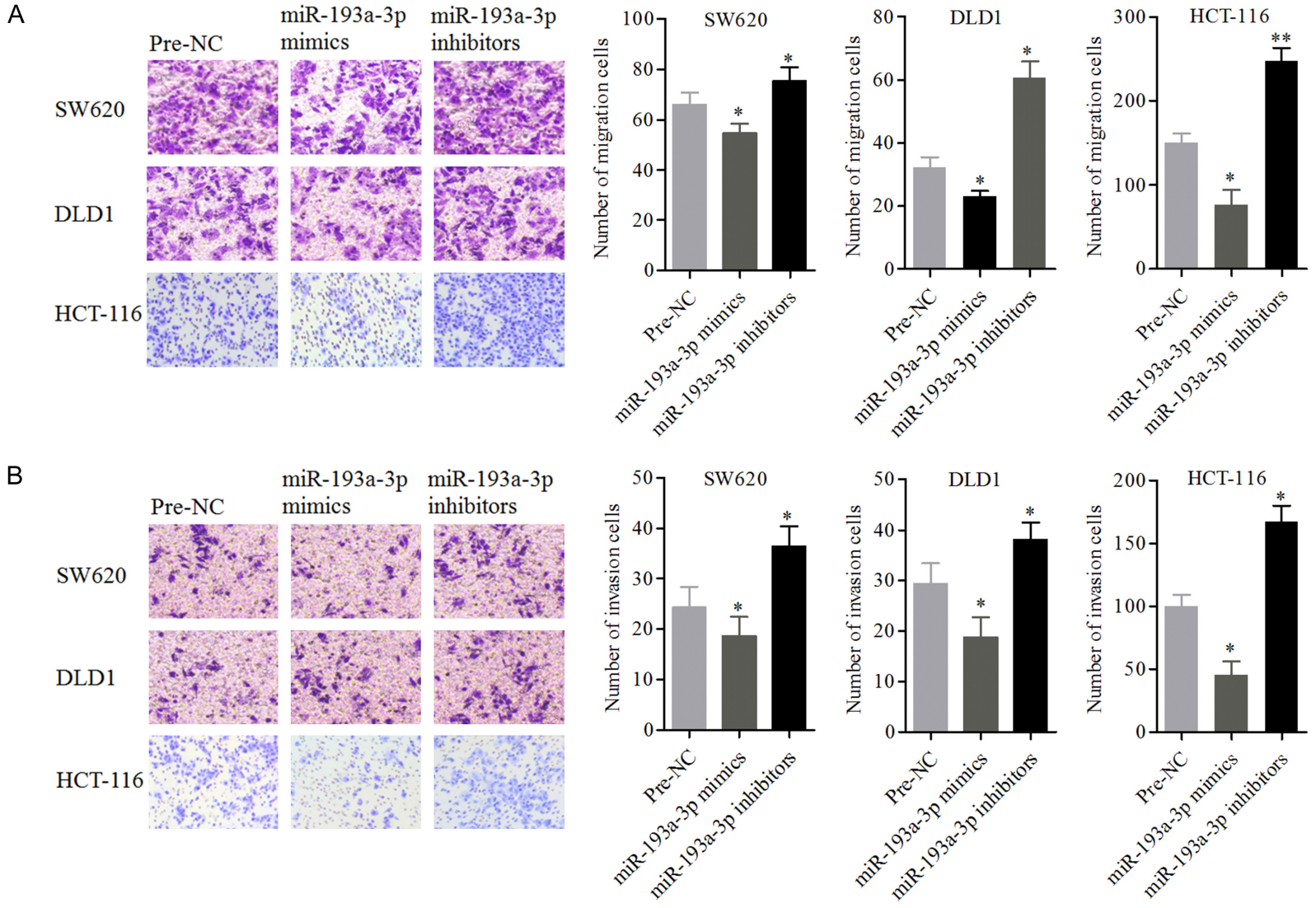
A
Pre-NC
miR-193a-3p mimics
miR-193a-3p inhibitors
SW620
DLD1
HCT-116
Number of migration cells
SW620
DLD1
HCT-116
Pre-NC
miR-193a-3p mimics
miR-193a-3p inhibitors
B
Number of invasion cells

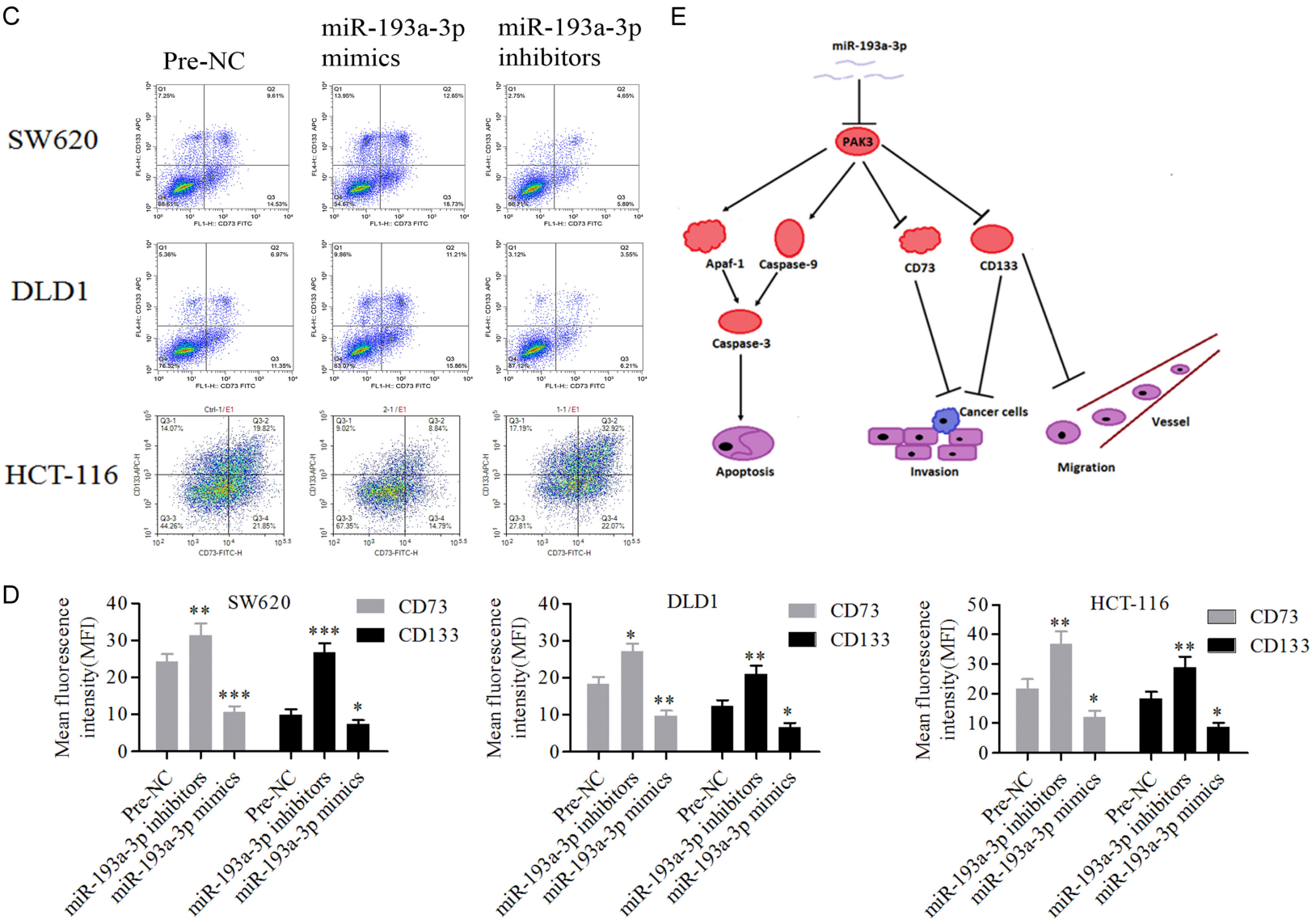

Figure 5. MiR193a-3p inhibited migration, invasion and the expression of CD73/CD133 in CRC cells. (A and B) Cell migration (A) and invasion (B) were inhibited by miR-193a-3p mimics and promoted by miR-193a-3p inhibitors. (C) The expression of CD73/133 molecules in CRC cells transfected with miR-193a-3p mimics and inhibitors. (D) Bar graphs of mean fluorescence intensities of CD73/133 in CRC cells. (E) A schematic model showing that miR-193a-3p expression in CRC leads to the activation of its target gene, PAK3, which contributes to the apoptosis of CRC by activating Apaf-1 and caspase-9 pathway and the restriction of metastasis of CRC by inhibiting the expression of CD73 and CD133. CRC cell lines: SW620, HCT116, DLD1. Statistical significance: $^{*}P<0.05$, $^{**}P<0.01$, $^{***}P<0.005$.

enzyme in apoptosis regulation [39]. Apoptotic protease activating factor-1 (Apaf-1) is engaged in the mitochondrial route or inherent of apoptosis, and upon the release of cytochrome c, oligomerizes into a large complex known as apoptosome. Procaspase-9, a mitochondrial initiator caspase, is initiated and stimulated by azotosome and thereby causes the processing of downstream caspase-3 [40]. Interestingly, we found that three proteins, caspase-3, caspase-9 and Apaf-1, were increased in miR-193a-3p mimics-transfected CRC cells.

In conclusion, the present study suggests that miR-193a-3p inhibits cell growth, migration, invasion, and induces cell apoptosis. PAK3 is validated as a novel target of miR-193a-3p in the progression of CRC. Our study uncovers that miR-193a-3p exerts suppressive function in CRC development by targeting PAK3 and schematically provides a new strategy to inhibit the PAK3-driven CRC progression. However, due to the limitation of sample size and distribution, the conclusion would be more appropriate after investigating more samples in the future.

Acknowledgements

This work was supported by the Scientific Research Projects from the Construction of Superiority Discipline Groups in Ningxia Medical University in 2017 (Grant No. XY201717).

Disclosure of conflict of interest

None.

Address correspondence to: Hui Yan, Tumor Hospital, General Hospital of Ningxia Medical University, Shengli Street, Xingqing District, Yinchuan 750004, Ningxia, People's Republic of China. Tel: +86-15109603181; E-mail: yan20200202@126.com

References

[1] Bray F, Ferlay J, Soerjomataram I, Siegel RL, Torre LA and Jemal A. Global cancer statistics 2018: GLOBOCAN estimates of incidence and mortality worldwide for 36 cancers in 185 countries. CA Cancer J Clin 2018; 68: 394-424.

[2] Ota M, Takamura N and Irimura T. Involvement of cell surface glycans in adhesion of human colon carcinoma cells to liver tissue in a frozen section assay: role of endo-β-galactosidase-sensitive structures. Cancer Res 2000; 60: 5261-5268.

[3] Kozovska Z, Gabrisova V and Kucerova L. Colon cancer: cancer stem cells markers, drug resistance and treatment. Biomed Pharmacother 2014; 68: 911-916.

[4] Chen W, Zheng R, Baade PD, Zhang S, Zeng H, Bray F, Jemal A, Yu XQ and He J. Cancer statistics in China, 2015. CA Cancer J Clin 2016; 66: 115-132.

[5] Torre LA, Bray F, Siegel RL, Ferlay J, Lortet-Tieulent J and Jemal A. Global cancer statistics, 2012. CA Cancer J Clin 2015; 65: 87-108.

[6] Fu D, Liu D, Zhang L and Sun L. Self-assembled fluorescent tripeptide nanoparticles for bioimaging and drug delivery applications. Chinese Chemical Letters 2020; 31: 3195-3199.

[7] Della Vittoria Scarpati G, Calura E, Di Marino M, Romualdi C, Beltrame L, Malapelle U, Troncone G, De Stefano A, Pepe S, De Placido S, D'Incalci M, Marchini S and Carlomagno C. Analysis of differential miRNA expression in primary tumor and stroma of colorectal cancer patients. Biomed Res Int 2014; 2014: 840921.

[8] Basnet S, Zhang ZY, Liao WQ, Li SH, Li PS and Ge HY. The prognostic value of circulating cell-free DNA in colorectal cancer: a meta-analysis. J Cancer 2016; 7: 1105-1113.

[9] Mendell JT and Olson EN. MicroRNAs in stress signaling and human disease. Cell 2012; 148: 1172-1187.

[10] Lin S and Gregory RI. MicroRNA biogenesis pathways in cancer. Nat Rev Cancer 2015; 15: 321-333.

[11] Adams BD, Kasinski AL and Slack FJ. Aberrant regulation and function of MicroRNAs in cancer. Curr Biol 2014; 24: R762-R776.

[12] Beermann J, Piccoli MT, Viereck J and Thum T. Non-coding RNAs in development and disease: background, mechanisms, and therapeutic approaches. Physiol Rev 2016; 96: 1297-1325.

[13] Rupaimoole R and Slack FJ. MicroRNA therapeutics: towards a new era for the management of cancer and other diseases. Nat Rev Drug Discov 2017; 16: 203-222.

[14] Friedman RC, Farh KK, Burge CB and Bartel DP. Most mammalian mRNAs are conserved targets of microRNAs. Genome Res 2009; 19: 92-105.

[15] Bartel DP. MicroRNAs: target recognition and regulatory functions. Cell 2009; 136: 215-233.

[16] Fu Y, Lin L and Xia L. MiR-107 function as a tumor suppressor gene in colorectal cancer by targeting transferrin receptor 1. Cell Mol Biol Lett 2019; 24: 31.

[17] Zhang N, Hu X, Du Y and Du J. The role of miRNAs in colorectal cancer progression and chemoradiotherapy. Biomed Pharmacother 2021; 134: 111099.

[18] Wei Y, Shao J, Wang Y, Shen H, Yu S, Zhang J and Yin L. Hsa-miR-370 inhibited P-selectin-induced cell adhesion in human colon adenocarcinoma cells. Mol Cell Biochem 2019; 450: 159-166.
[19] Zhao L, Yu J, Wang J, Li H, Che J and Cao B. Isolation and identification of miRNAs in exosomes derived from serum of colon cancer patients. J Cancer 2017; 8: 1145-1152.
[20] Wang P, Zou F, Zhang X, Li H, Dulak A, Tomko RJ, Lazo JS, Wang Z, Zhang L and Yu J. microRNA-21 negatively regulates Cdc25A and cell cycle progression in colon cancer cells. Cancer Res 2009; 69: 8157-8165.
[21] Cui X, Liu X, Han Q, Zhu J, Li J, Ren Z, Liu L, Luo Y, Wang Z, Zhang D, Fan Y, Zhang D and Dong G. DPEP1 is a direct target of miR-193a-5p and promotes hepatoblastoma progression by PI3K/Akt/mTOR pathway. Cell Death Dis 2019; 10: 701.
[22] Ju B, Nie Y, Yang X, Wang X, Li F, Wang M, Wang C and Zhang H. miR-193a/b-3p relieves hepatic fibrosis and restrains proliferation and activation of hepatic stellate cells. J Cell Mol Med 2019; 23: 3824-3832.
[23] He H and Baldwin GS. p21-activated kinases and gastrointestinal cancer. Biochim Biophys Acta 2013; 1833: 33-39.
[24] Yang H, Fang F, Chang R and Yang L. MicroRNA-140-5p suppresses tumor growth and metastasis by targeting transforming growth factor β receptor 1 and fibroblast growth factor 9 in hepatocellular carcinoma. Hepatology 2013; 58: 205-217.
[25] Goldberger N, Walker RC, Kim CH, Winter S and Hunter KW. Inherited variation in miR-290 expression suppresses breast cancer progression by targeting the metastasis susceptibility gene Arid4b. Cancer Res 2013; 73: 2671-2681.
[26] Pu Y, Zhao F, Cai W, Meng X, Li Y and Cai S. MiR-193a-3p and miR-193a-5p suppress the metastasis of human osteosarcoma cells by down-regulating Rab27B and SRR, respectively. Clin Exp Metastasis 2016; 33: 359-372.
[27] Livak KJ and Schmittgen TD. Analysis of relative gene expression data using real-time quantitative PCR and the 2-ΔΔCT method. Methods 2001; 25: 402-408.
[28] Morgado AL, Rodrigues CM and Solá S. MicroRNA-145 regulates neural stem cell differentiation through the Sox2-Lin28/let-7 signaling pathway. Stem Cells 2016; 34: 1386-1395.
[29] Ghosh A, Dasgupta D, Ghosh A, Roychoudhury S, Kumar D, Gorain M, Butti R, Datta S, Agarwal S, Gupta S, Krishna Dhali G, Chowdhury A, Schmittgen TD, Kundu GC and Banerjee S. MiRNA199a-3p suppresses tumor growth, migration, invasion and angiogenesis in hepatocellular carcinoma by targeting VEGFA, VEGFR1, VEGFR2, HGF and MMP2. Cell Death Dis 2017; 8: e2706.
[30] Lagos-Quintana M, Rauhut R, Meyer J, Borkhardt A and Tuschl T. New microRNAs from mouse and human. RNA 2003; 9: 175-179.
[31] Xu C, Liu S, Fu H, Li S, Tie Y, Zhu J, Xing R, Jin Y, Sun Z and Zheng X. MicroRNA-193b regulates proliferation, migration and invasion in human hepatocellular carcinoma cells. Eur J Cancer 2010; 46: 2828-2836.
[32] Mets E, Van der Meulen J, Van Peer G, Boice M, Mestdagh P, Van de Walle I, Lammens T, Goossens S, De Moerloose B, Benoit Y, Van Roy N, Clappier E, Poppe B, Vandesompele J, Wendel HG, Taghon T, Rondou P, Soulier J, Van Vlierberghe P and Speleman F. MicroRNA-193b-3p acts as a tumor suppressor by targeting the MYB oncogene in T-cell acute lymphoblastic leukemia. Leukemia 2015; 29: 798-806.
[33] Wang L, Zhang Y, Zhao L, Liu S, Yu S, Ma Y and Sun G. MicroRNA-193b inhibits the proliferation, migration and invasion of gastric cancer cells via targeting cyclin D1. Acta Histochem 2016; 118: 323-330.
[34] Liu RX, Wang WQ, Ye L, Bi YF, Fang H, Cui B, Zhou WW, Dai M, Zhang J, Li XY and Ning G. p21-activated kinase 3 is overexpressed in thymic neuroendocrine tumors (carcinoids) with ectopic ACTH syndrome and participates in cell migration. Endocrine 2010; 38: 38-47.
[35] Eswaran J, Lee WH, Debreczeni JÉ, Filippakopoulos P, Turnbull A, Fedorov O, Deacon SW, Peterson JR and Knapp S. Crystal structures of the p21-activated kinases PAK4, PAK5, and PAK6 reveal catalytic domain plasticity of active group II PAKs. Structure 2007; 15: 201-213.
[36] de Leve S, Wirsdörfer F and Jendrossek V. Targeting the immunomodulatory CD73/adenosine system to improve the therapeutic gain of radiotherapy. Front Immunol 2019; 10: 698.
[37] Li Z. CD133: a stem cell biomarker and beyond. Exp Hematol Oncol 2013; 2: 17.
[38] Avrutsky MI and Troy CM. Caspase-9: a multimodal therapeutic target with diverse cellular expression in human disease. Front Pharmacol 2021; 12: 701301.
[39] Lossi L, Castagna C and Merighi A. Caspase-3 mediated cell death in the normal development of the mammalian cerebellum. Int J Mol Sci 2018; 19: 3999.
[40] Shakeri R, Kheirollahi A and Davoodi J. Apaf-1: regulation and function in cell death. Biochimie 2017; 135: 111-125.

Table S1. The sequences of siRNAs, mimics and inhibitors for cell transfection

siRNAs	sense	antisense
PAK3	5'-GCAACCCAAGAAGGAAUUATT-3'	5'-UAAUUCCUUCUUGGGUUGCTT-3'
miR-193a-3p	5'-AACUGGCCUACAAAGUCCCAGU-3'	5'-UGGGACUUUGUAGGCCAGUUUU-3'

Table S2. The forward and reverse primer sequences for RT-qPCR

Primers	forward	reverse
PAK3	5' CACTCAAACCAGGTGATCCATAG 3'	5' CCACCATAGTGCTTCGTTTACT 3'
miR-193a-3p	5'-TTTGAGGGATATTTAGAGTTT-3'	5'-AACCTAAAAAACAACCTAACC-3'
U6	5'-CTCGCTTCGGCAGCACA-3'	5'-AACGCTTCACGAATTTGCGT-3'

Table S3. The forward and reverse primer sequences for luciferase assays

forward	reverse
5' GGGTACCCAATGCCCAGCTTGTCAGCCATA 3'	5' CCTCGAGGGTTCCTGTCCTCGTTAAACCAT 3'

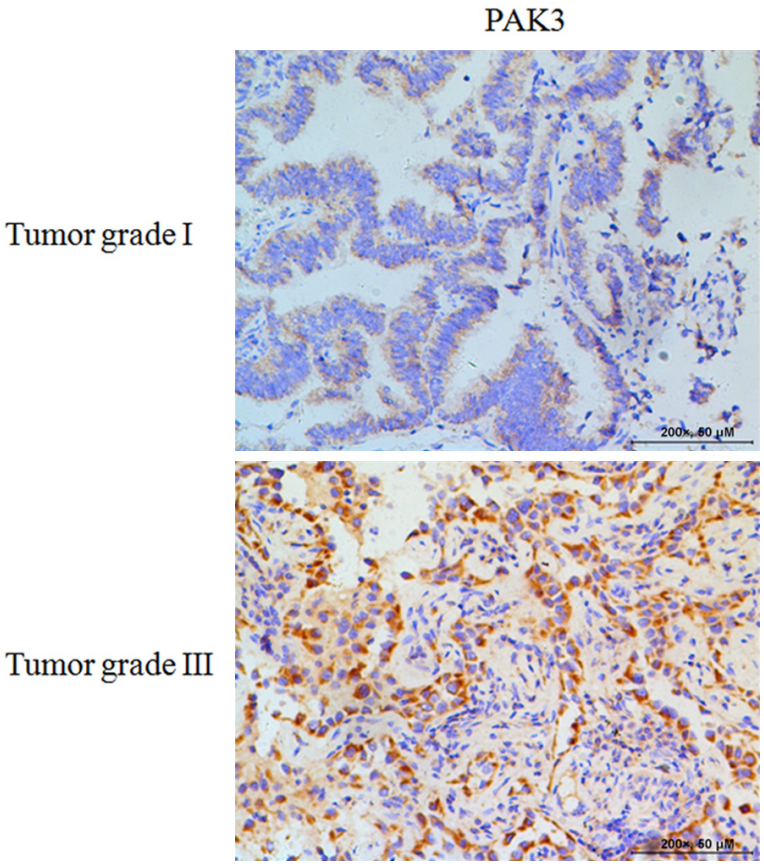

Figure S1. The protein levels of PAK3 in CRC tissues from tumor grade I and tumor grade II showed that PAK3 proteins were increased in CRC samples.